DESIGN OF A 2.7 GHZ LINEAR OTA IN BIPOLAR TRANSISTOR-ARRAY TECHNOLOGY WITH LATERAL PNPS

Adam Wyszynski, Rolf Schaumann, Stanislaw Szczepanski and Paul Van Halen*

Department of Electrical and Computer Engineering
Portland State University, P.O. Box 751,
Portland, Oregon, 97207-0751, U.S.A

* The Institute of Electronic Technology
Technical University of Gdansk, Poland

Abstract - The design of a tunable high-frequency fully integrated bipolar operational transconductance amplifier (OTA) is presented. Techniques resulting in tunability and broadbanding are discussed, as well as unavoidable trade-offs resulting from the lack of a vertical *pnp* device. Using an 8 *GHz* bipolar transistor array process, the OTA has a -3 *dB* frequency of more than 2.7 *GHz*, a maximum linear input range of ± 2.5 *V*, and dissipates 28 *mW* for a power supply of ± 5 *V*. Two applications of the OTA in OTA-C filter design are presented briefly.

I. INTRODUCTION

For integrated circuit signal processing applications at very high frequencies, such as continuous-time filters at several hundred megahertz, ultra fast operational transconductance amplifiers (OTAs) are required. Because so far, bipolar technology seems to be superior in this field, combining high speed and good linearity with a proven and inexpensive process [1], [2], this paper describes a high-frequency bipolar fully differential operational transconductance amplifier (OTA). Recently, fast OTAs in CMOS technology have also been reported [3] - [5] but their frequency range is still inferior to that of bipolar designs. BiCMOS technology has potential for giving faster OTAs than CMOS [6] but it cannot match the performance of bipolar technology as the latter has inherently faster devices. On the other hand, chip area, and speed versus power are much better in BiCMOS than in bipolar technology, which makes BiCMOS particularly promising for analog and mixed digital/analog applications. GaAs technology, although theoretically much faster than bipolar, has not yet overcome a number of obstacles [7], [8], preventing it from yielding applications that can take full advantage of its speed.

II. OTA CIRCUIT DESCRIPTION

A. Transconductance Cell

The schematic diagram of the OTA with common-mode feedback (CMF) is presented in Fig. 1. The circuit consists of two current-coupled differential pairs. Transistors Q_1, Q_2 in the inner pair are biased from the tail current source I_{E1} and work with a local series feedback formed by the resistors R_1 and diodes Q_3, Q_4. This results in the desired wide linear range of a maximum of ± 2.5 *V*. Transistors Q_5, Q_6 in the outer pair are biased from the separate tail current source I_{E2}. For reasons to be discussed below, I_{E2} is kept constant whereas I_{E1} is made to vary to allow tuning of the transconductance g_m.

The bipolar process has low Early voltages (28 *V* for *npn* and 23 *V* for *pnp* devices) which results in fairly low output resistances of transistors Q_5, Q_6 and Q_9, Q_{10}. To improve the output resistance of the OTA, a cascode output stage with transistors Q_7, Q_8 is used. High output impedance of *pnp* sources is achieved by emitter degeneration in transistors Q_9 and Q_{10}. For the lateral *pnp* transistors this solution proved to be superior to cascode or Wilson sources as far as the output impedance, temperature behavior and output parasitic capacitances are concerned.

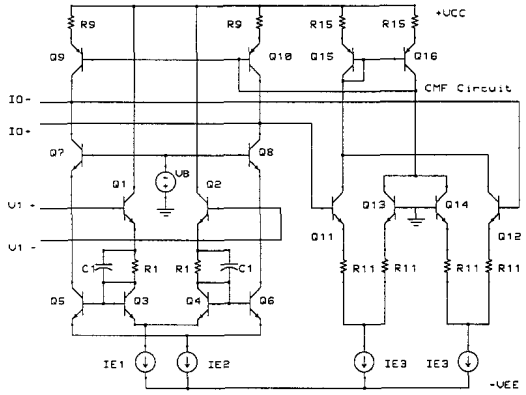

Fig. 1. Fully-tunable bipolar OTA with CMF circuit.

B. Transconductance

With increasing emitter degeneration the linear range of the input stage in Fig. 1 is extended for the price of a decreasing transconductance value. Noting that the $i_C - v_{BE}$ relationship of a forward biased transistor is $i_C \approx I_S exp(v_{BE}/V_T)$, where I_S is the saturation current, $V_T = kT/q$ is the thermal voltage, and assuming $g_{m3}R_1 \gg 1$ and $g_{m1}R_1 \gg 1$, the transconductance of the input stage is

$$g_{m1}{}^{*} = \frac{\partial i_{C1}}{\partial v_{in}} = \frac{g_{m1}}{2(1+g_{m1}R_1)} \approx \frac{1}{2R_1} \tag{1}$$

With $I_{C1} = I_{E1}/2$, the transconductance g_{m1} of transistor Q_1 (or Q_2) can be directly related to its bias current as

$$g_{m1} = \partial i_{C1}/\partial v_{BE1} = I_{E1}/(2V_T) \tag{2}$$

From (1) it follows that $g_{m1}{}^{*}$ is approximately constant and no tuning of the first stage is possible. In order to implement the necessary electronic tuning, a second stage is introduced. As seen from Fig. 1, transistors Q_3 and Q_5 have different bias currents, but there is a current *signal* path from Q_3 to Q_5. The transconductance of the second stage is equal to that of Q_5 and can be written as

$$g_{m5} = \partial i_{C5}/\partial v_{BE5} = I_{E2}/(2V_T) \tag{3}$$

Neglecting the base current of Q_7, the total transconductance g_m is defined by

$$g_m = i_{out}/v_{in} \approx \partial i_{C5}/\partial v_{in} \tag{4}$$

With (1), (2) and (3), eq. (4) can be expressed as

$$g_m \approx \frac{\partial i_{C5}}{\partial v_{BE5}} \frac{\partial v_{BE5}}{\partial v_{in}} \frac{\partial i_{C1}}{\partial i_{C1}} = \frac{\partial i_{C1}}{\partial v_{in}} \frac{\partial i_{C5}/\partial v_{BE5}}{\partial i_{C3}/\partial v_{BE3}} = g_{m1}{}^{*} \frac{g_{m5}}{g_{m3}} \tag{5}$$

where $I_{C1} \approx I_{C3}$ was applied and it was noted that $\partial v_{BE5} = \partial v_{BE3}$ because the emitter nodes of both Q_3 and Q_5 are at *ac* ground. Thus it follows with (1) that the total transconductance equals

$$g_m = 1/(2R_1)\, I_{C5}/I_{C3} = 1/(2R_1)\, I_{E2}/I_{E1} \tag{6}$$

0-7803-0593-0/92 $3.00 1992 IEEE

which indicates that either of the currents I_{E1}, I_{E2} or both can be used for tuning g_m. The best results for high output impedance and stability of V_{out} with tuning, temperature and supply variation are achieved when I_{E2} is fixed and I_{E1} is varied, because the current gain β of lateral *pnp* transistors falls quickly with increasing bias. This in turn lowers their output impedance, see (8), which results in degradation of quality factors of any filter built with the transconductor. For the same reasons a stable *dc* output level is achieved

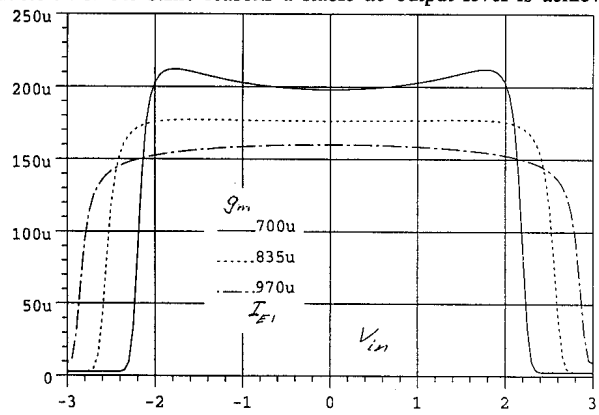

Fig. 2. Transconductance g_m in S of the bipolar OTA in Fig. 1.

when I_{E2} is fixed. The results of SPICE simulations for tuning of g_m are presented in Fig. 2. Observe from (6) that g_m can readily be made insensitive to temperature and certain process tolerances of R_1 by making I_{E1} inversely proportional to a resistor of the same type and technology as R_1: g_m then depends only on a resistor ratio, the fixed current I_{E2} and a supply voltage.

C. Input and Output Impedance

The input and output impedances of an OTA must be kept as high as possible as they lower the quality factors of the integrators and filters built with the OTA. In the present case, the differential input impedance for low frequencies is increased by the emitter resistors R_1 of the input transistors Q_1, Q_2 as

$$R_{in} = 2[r_{\pi 1}(1 + g_{m1}R_1)] \approx 2\beta_1 R_1 \tag{7}$$

where $r_{\pi 1}$ is the input resistance of Q_1 and $r_{\pi 1} g_{m1} = \beta_1$.

The differential output impedance is a parallel connection of the output impedances of the cascode configuration Q_5, Q_7 and Q_6, Q_8 and of the load devices Q_9, Q_{10}. The common-mode feedback (CMF) to be discussed below lowers this value. Without CMF, the differential output impedance for low frequencies is given by

$$R_{out} = 2r_7 r_9/(r_7 + r_9) \approx 2r_9 \tag{8}$$

where $r_7 \approx \beta_7 r_{o7}$ is the output impedance of the cascode stage $Q_5 - Q_7$, $r_9 \approx r_{o9}[1 + g_{m9}(r_{\pi 9} \| R_9)] \approx r_{o9}(1 + \beta_9)$ is the total output impedance of the load *pnp* transistor Q_9 with emitter degeneration, and r_{o7}, r_{o9} are the output impedances of transistors Q_5, Q_7. Note that increasing resistor R_9 above a certain value does not affect r_9 because $r_{\pi 9} = \beta_9 / g_{m9} \ll R_9$ due to the low value of β of *pnp* transistors.

D. Linearity

With the use of emitter degeneration, the linear range is extended from $\pm V_T$ to a maximum of ± 2.5 V. The linear range could be wider except for the need of the cascode output. The linearity of the transconductance is indicated in Fig. 3; the linearity error ε, defined as

$$\varepsilon = \frac{I_{out} - g_m(0)V_{in}}{I_{E1} + I_{E2}} 100\ \% \tag{9}$$

is less than ± 0.05 % in the region ± 2.33 V. I_{out} is the output current, $g_m(0)$ is the value of g_m for $V_{in} = 0$, V_{in} is the input voltage, and $I_{E1} + I_{E2}$ is the bias current of the OTA (see Fig. 1).

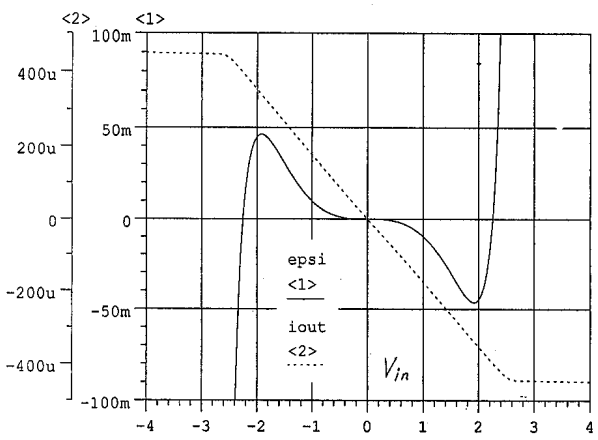

Fig. 3. <1> Linearity error as percentage of total DC bias current, <2> DC transfer curve of the output current I_{out}.

E. Common-Mode Feedback (CMF) Circuit

The CMF circuit in Fig. 1 is a modification of prior designs [9]. Table 1 shows the result of the CMF scheme; the modification from [9] worked towards high input impedance, wide dynamic range, low power consumption, and stable output voltage with temperature and power supply variation. It has been obtained by using *npn* and *pnp* devices with emitter degeneration. In this configuration, a wide linear range of the CMF circuit is obtained that is adequate for the dynamic range of the OTA.

Table 1. V_{out} *Variation*

Parameter	Range	V_{out}
load	1 Ω to 100 kΩ	≈ 0 *mV*
tuning I_{E1}	400 μA to 750 μA	≈ 0 *mV* to − 2 *mV*
temperature	− 30 °C to + 100 °C	− 23 *mV* to + 5*mV*
power supply	± 4.5 *V* to ± 7.5 *V*	− 31 *mV* to + 47*mV*

III. BANDWIDTH EXTENSION AND COMPENSATION

The signal to be processed in the OTA is current. The signal path consists of four different transistor configurations: common-collector, a diode (impedance transformer), common-emitter, and common-base. After performing all required functions, the signal current is directed to the output.

A. Frequency Response of the Input Stage

The input transistor Q_1 works as emitter follower with emitter load R_1, but with no collector load R_C. Therefore, the Miller capacitance C_{M1} given by

$$C_{M1} = (1 + g_{m1}R_C)C_{\mu 1} \approx C_{\mu 1} \tag{10}$$

is reduced to that of $C_{\mu 1}$, so there is no Miller effect on the frequency response of transistor Q_1.

Referring to the small-signal model in Fig. 4 and assuming that $r_{bb5} \approx 0$, $g_{m3} \gg 1/r_{\pi 5}$ and $g_{m3}R_1 \gg 1$, the impedance Z_E seen from the emitter of Q_1 can be approximated by

$$Z_E \approx R_1 + 1/[g_{m3} + s(C_{\pi 3} + C_{\pi 5})] \approx R_1 \tag{11}$$

Referring to Fig. 1, the common-emitter connected Q_5 loaded with a common-base connected Q_7 forms the cascode configuration. For low frequencies, neglecting r_{bb7}, the input impedance of Q_7 is approximately $1/g_{m7}$. This forms a small load in the collector of Q_5, and with respect to (10) written for transistor Q_5, results in a Miller capacitance of this transistor of only $2C_{\mu 5}$. Note that high R_1 buffers Q_1 from the effects of Q_3 and Q_5.

Referring to Fig. 4, neglecting the source resistor R_S, the base resistance r_{bb1}, the output resistance r_{o1}, the collector-base capacitance $C_{\mu 1}$, and the collector-substrate capacitance C_{CS1} of Q_1, and assuming $g_{m1}R_1 \gg 1$, the current through R_1 is approximated by

$$I_1 \approx V_{in}\frac{g_{m1} + sC_{\pi 1}}{(1 + g_{m1}R_1) + sR_1C_{\pi 1}} \approx \frac{V_{in}}{R_1} \tag{12}$$

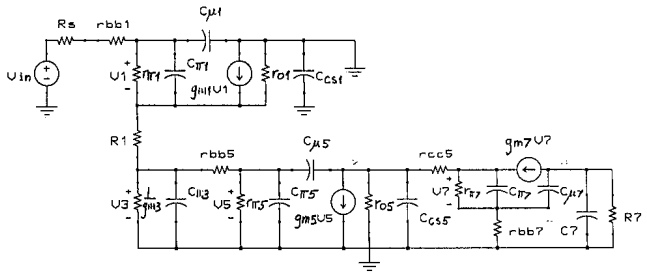

Fig. 4. Small-signal model for the bipolar OTA in Fig. 1.

From (12) it follows that in the range of interest (one decade below f_T), for large values of R_1, I_1 is approximately independent of frequency. The results of SPICE simulations confirm the predicted results for higher values of R_1 (above $1k\Omega$).

B. Frequency Response of the Intermediate Stage

Leaving Q_1, the signal travels through a diode-connected transistor Q_3, and then into base of the current-coupled Q_5. It can be seen from Fig. 4, that the small resistance $1/g_{m3}$ of the diode Q_3 shunts the input impedance of Q_5, improving thereby its -3 *dB* frequency, because $1/g_{m3} \ll r_{bb5} \ll r_{\pi 5}$. The collector current of Q_5 can be derived as a two-pole function,

$$I_5 = -g_{m5}V_5 \approx -\frac{g_{m5}}{g_{m3}}\frac{V_{in}}{R_1}\frac{1}{(1+s/p_1)(1+s/p_2)} \tag{13}$$

whose pole location can be estimated as

$$|p_1| > g_{m3}/C_{\pi 3}, \tag{14}$$

which is greater than f_T of Q_5, and

$$(C_{\pi 3}+C_{\pi 5})/(r_{bb5}C_{\pi 3}C_{\pi 5}) > |p_2| > 1/(r_{bb5}C_{\pi 5}) \tag{15}$$

The presence of the resistance r_{bb5} introduces the dominant pole of Q_5 close to f_T.

C. Frequency Response of the Output Stage

Referring to Fig. 4, the collector current of the cascode output transistor Q_7 can be approximated by a two-pole function as

$$I_7 = g_{m7}V_7 \approx \frac{I_5}{(1+s/p_3)(1+s/p_4)} \tag{16}$$

The analysis of the frequency response of the output stage shows that depending on g_{m7}, which is directly proportional to the bias current I_{E2}, the output stage can have two real or two conjugate complex poles. Because complex poles add to phase shift and can lead to instability, attention should be paid not to increase I_{E2} above phase margin limits. Note though that for designing a high-frequency filter, the transconductance should be as high as possible since the cut-off frequency is proportional to g_m. This may force to increase I_{E2} so that two complex poles are present. On the other end, low current I_{E2} results in lower frequency of the dominant pole. The maximum is obtained when the two poles have the same value. This gives the highest frequency with no additional phase shift due to complex poles. The double pole can be derived as

$$s = -p_{3,4} \approx \frac{C_{\pi 7}+C_{CS5}}{2C_{\pi 7}C_{CS5}(r_{cc5}+r_{bb7})} \tag{17}$$

It is the dominant pole of the whole OTA, caused by the time constant of the collector-substrate capacitance C_{CS5}, in series with $C_{\pi 7}$, and by the parasitic series resistances r_{cc5}, r_{bb7}.

The cascode stage extends the bandwidth, substantially improves the output impedance of the OTA, and buffers the output from the rest of the circuit. The result of SPICE simulations for the frequency response of the whole OTA are shown in Fig. 5.

Increasing the number of stages improves the performances of the OTA at the cost of introducing poles and increasing the total phase shift. From (13) and (16) it follows that there are at least four main poles associated with all stages, but because they are higher than or located close to f_T, the final -3 *dB* frequency of the output current is more than 2.7 *GHz* with $f_T = 8$ *GHz*.

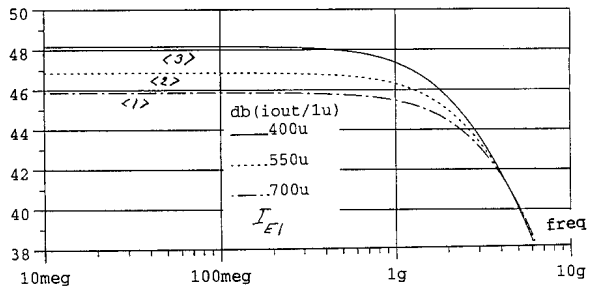

Fig. 5. Frequency response of the bipolar OTA in Fig. 1, I_{E1} is a parameter. – 3 *dB* frequencies are: <1> 3187 *MHz*, <2> 2704 *MHz*, <3> 2223 *MHz*.

D. Excess Phase Compensation

To avoid errors in Q-factor of a high-frequency filter, in the frequency range of interest the phase ϕ of an OTA must normally not deviate by more than a fraction of a degree from its ideal. This requires compensation of the phase change well before the -3 *dB* frequency of the OTA. It was shown earlier that the transconductance has four main poles of which $p_{3,4}$ is dominant. Thus, the frequency response can be approximated by this dominant pole, and the effect of the remaining poles will be modeled by a phase error $-\omega\tau$, i.e.

$$g_m(s) \approx g_{m0}\frac{e^{-s\tau}}{(1+s/p_{3,4})} \tag{18}$$

Further note that in the frequency range of any applications of interest $\omega \ll p_{3,4}$ so that a reasonable model is

$$g_m(s) \approx g_{m0}e^{-s\tau} \approx g_{m0}(1-s\tau) \approx \frac{g_{mo}}{1+s\tau} \tag{19}$$

In (19), τ may also represent any relevant phase contribution of the dominant pole at $-p_{3,4}$. Using (6) yields

$$g_m \approx \frac{I_{E2}}{I_{E1}}\frac{1}{2R_1}\frac{1}{(1+s\tau)} \tag{20}$$

Excess phase compensation requires canceling the term $1+s\tau$ in the denominator of (20); it is achieved by placing a small capacitor C_1 in parallel with R_1 as is shown in Fig. 1, to yield

$$g_m \approx \frac{I_{E2}}{I_{E1}}\frac{1+sR_1C_1}{2R_1}\frac{1}{(1+s\tau)} \tag{21}$$

Cancellation is obtained for

$$C_1 = \tau(\omega)/R_1 \tag{22}$$

Note that τ, as indicated, is generally a function of frequency so that excess phase compensation in a wider range of frequencies would require C_1 to be a function of frequency. In spite of this restriction, the simple compensation scheme for the main phase errors is satisfactory as shown in Fig. 6, Curves 1,2,3. In practice, electronic fine adjustment is necessary to permit automatic tuning of Q-factor errors caused by excess phase. A convenient technique for achieving this requirement combines the capacitor C_1 with the bias-dependent capacitor of the cascode transistors Q_7 and Q_8.

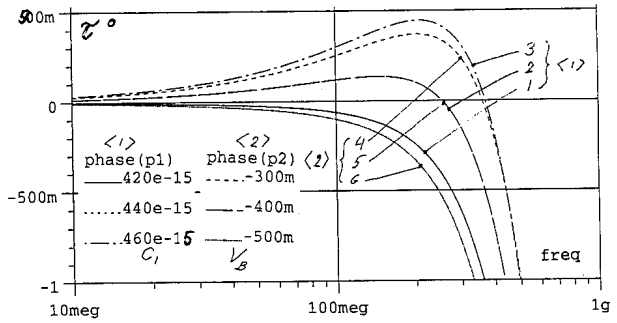

Fig. 6. Excess phase of the bipolar OTA in Fig. 1.

The idea of the cascode fine-tuning is straightforward: if a tunable instead of a fixed source V_B (see Fig. 1) is used, the base potential of Q_7 varies. Because the collector potential V_{C7} of Q_7 is held at 0 V by the CMF circuit, and V_{BE5} and V_{BE7} are fixed by the bias current I_{E2}, changes in V_B affect only V_{BC7} and V_{BC5}, thereby changing the collector-base and collector-substrate capacitances of Q_5 and Q_7.

From (17) it is seen that the poles of the output stage depend on the collector-substrate capacitance C_{CS5}. Assuming that the substrate is at 0V, the collector-substrate voltage of Q_5 is

$$V_{CS5} = V_{C5} - 0V = V_B - V_{BE7} \tag{23}$$

For an abrupt doping profile of the collector-substrate junction, C_{CS5} can be written as

$$C_{CS5} = C_{CS0}/\sqrt{1 + V_{CS5}/\Phi} = C_{CS0}/\sqrt{1 + (V_B - V_{BE7})/\Phi} \tag{24}$$

where Φ is the built-in potential of the junction and C_{CS0} is the value of C_{CS5} at $V_{CS5} = 0V$. From (24) and (17) it follows that by increasing V_B, C_{CS5} decreases and the poles $p_{3,4}$ move towards higher frequencies. The effect of this small shift of $p_{3,4}$ on excess phase is the same as an increase of C_1. By this method accurate electronic adjusting of excess phase is accomplished. The results of SPICE simulations are presented in Fig. 6, Curves 4,5,6.

VI. CONCLUSIONS

A high-frequency bipolar linear transconductance amplifier has been presented. The circuit dissipates 16 mW for ±3.5V, the lowest possible power supply voltage, and 28 mW for a power supply of ±5 V. The realization uses emitter degeneration to obtain a wide linear input range up to more than ±2.5V. The OTA is fully tunable by using the second stage to obtain different bias currents and different g_m-values, so that g_m can be changed in the range up to 50% of its original value. The cell can be designed for any value of g_m from μS to mS, and finds a broad scope of applications both for low and high frequencies. The –3 dB frequency of the OTA is more than 2.7 GHz, which has been achieved with lateral pnp devices as current source loads. A suitable technique has been found, which allows to adjust phase compensation electronically. This may be applied in an automatic Q tuning scheme. The technique is based on shifting the poles of the cascode connected output stage by modifying its capacitances. The traditional fixed frequency compensation is used in parallel.

To illustrate applications of the above OTA, two filters have been designed. In both designs, in order to save the number of components and the total power dissipated, double-input OTAs [10] derived directly from the above OTA by adding an extra pair of input transistors with their emitter resistors, have been applied.

In Fig. 7 the simulated transfer functions of a 75 MHz 7-th order Bessel filter with and without an additional zero in the stopband and with zero and equalization boost are presented. Contrary to the design in [1] using a voltage amplifier, the equalization

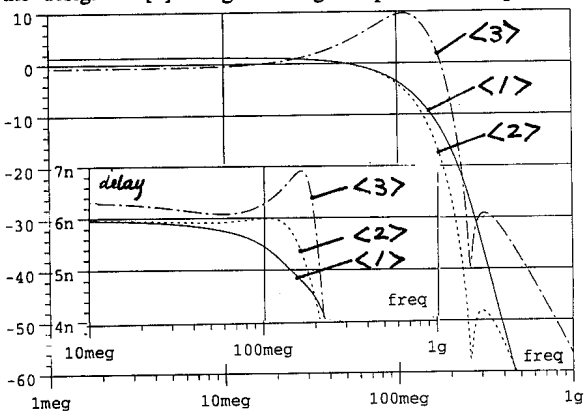

Fig. 7. Simulated transfer functions of a 75 MHz 7-th order Bessel filter. <1> without zero, <2> with a zero in the stopband, <3> with zero and equalization boost. Group delay characteristics are in the detail below.

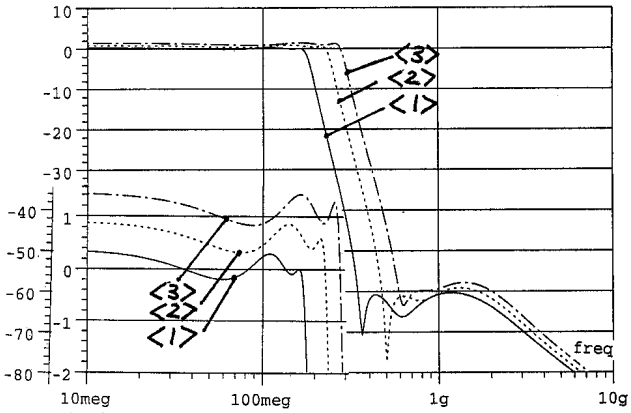

Fig. 8. Simulated transfer functions of a 250 MHz 5-th order elliptic filter. <1> f_c = 168 MHz, <2> f_c = 224 MHz, <3> f_c = 270 MHz. Passband detail below.

(boost) of 10 dB has been achieved with the use of a special boost OTA, using current injection. Putting a zero in the stopband allows a steeper roll-off of the transfer function. Additionally, as shown in Fig. 7, the zero extends the flat range of group delay up to 130 MHz. The non-ideal delay obtained with boost and compensation zero can be attributed to the finite R_{out} of the OTAs. The filter can be tuned in the range of 54 - 100 MHz.

As the second application for VHF range, a 250 MHz 5-th order elliptic filter with 0.5 dB ripple and -55 dB attenuation has been design. Its simulated transfer functions are presented in Fig. 8. The simulated RLC ladder filter has been realized using six double-input OTAs only. The filter is tunable in the range of 168 - 270 MHz.

Acknowledgments - This work was supported in part by a 1991/1992 Tektronix Fellowship and by the Kosciuszko Foundation.

REFERENCES

[1] G. A. DeVeirman and R. Yamasaki, "Monolithic 10 - 30 MHz Bipolar Bessel Lowpass Filter," *Proc. IEEE Int. Symp. Circ. Syst.*, pp. 1444-1447, 1991.

[2] T. Yanagisawa, "Trends of Active Filters in the VHF Range," *Proc. IEEE Int. Symp. Circ. Syst.*, pp. 1737-1740, 1991.

[3] B. Nauta and E. Seevinck, "110 MHz CMOS Transconductance-C Lowpass Filter, " *Dig. Tech ESSCIRC*, pp. 141-144, 1989.

[4] M. Ismail, R. Wassenaar, and W. Morrison, "A High-Speed Continuous-Time Bandpass VHF Filter in MOS Technology," *Proc. IEEE Int. Symp. Circ. Syst.*, pp. 1761-1764, 1991.

[5] S. Szczepanski, A. Wyszynski, and R. Schaumann, "Highly Linear Voltage-Controlled CMOS Transconductors," submitted to IEEE Transactions on Circuit and Systems, 1991.

[6] R. Castello, F. Montecchi, R. Alini, and A. Baschirotto, "A Very Linear BiCMOS Transconductor for High-Frequency Filtering Applications," *Proc. IEEE Int. Symp. Circ. Syst.*, pp. 1364-1367, 1990.

[7] P. Wu and R. Schaumann, "A High-Frequency GaAs Transconductance Circuit and Its Applications," *Proc. IEEE Int. Symp. Circ. Syst.*, pp. 3081-3084, 1990.

[8] C. Toumazou and D. G. Haigh "Integrated Microwave Continuous-Time Active Filters Using Fully Tunable GaAs Transconductors," *Proc. IEEE Int. Symp. Circ. Syst.*, pp. 1765-1768, 1991.

[9] P. Wu, R. Schaumann, and P. Latham, "Design Considerations for Common-Mode Feedback Circuits in Fully-Differential Operational Transconductance Amplifiers with Tuning," *Proc. IEEE Int. Symp. Circ. Syst.*, pp. 1363-1366, 1991.

[10] A. Wyszynski and R. Schaumann, "Using Multiple-Input Transconductors to Reduce the Number of Components in OTA-C Filter Design," *Elect. Lett.*, Vol. 28, 3/1992.